NAIC-ID(RS)T-0076-96

NATIONAL AIR INTELLIGENCE CENTER

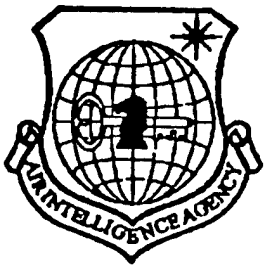

INTERFERENCE DIAGNOSIS OF LASER
INDUCED VAPOR PLUME

by

Yuan Yonghua, Liu Changling, et al.

**Approved for public release:
distribution unlimited**

DISCLAIMER NOTICE

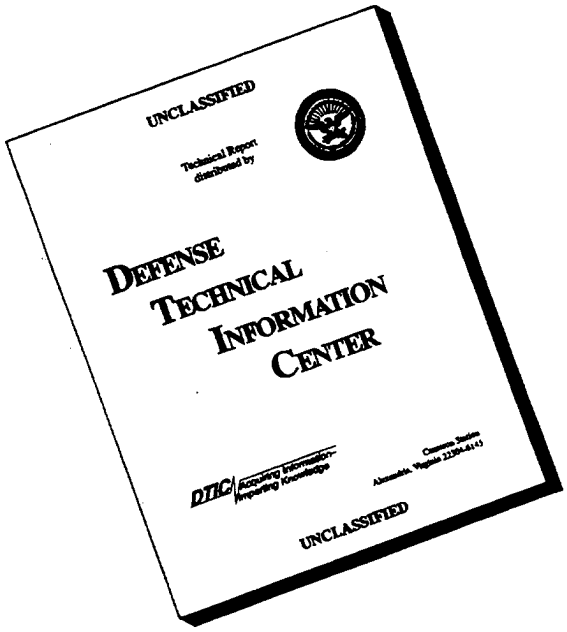

THIS DOCUMENT IS BEST QUALITY AVAILABLE. THE COPY FURNISHED TO DTIC CONTAINED A SIGNIFICANT NUMBER OF PAGES WHICH DO NOT REPRODUCE LEGIBLY.

HUMAN TRANSLATION

NAIC-ID(RS)T-0076-96 22 April 1995

MICROFICHE NR: 96C000335

INTERFERENCE DIAGNOSIS OF LASER INDUCED VAPOR PLUME

By: Yuan Yonghua, Liu Changling, et al.

English pages: 11

Source: Gaoya Wuli Xuebao (Chinese Journal of High Pressure Physics), Vol. 6, Nr. 1, March 1992; pp. 23-29

Country of origin: China
Translated by: SCITRAN
F33657-84-D-0165
Requester: NAIC/TATD/Bruce Armstrong
Approved for public release: distribution unlimited.

GRAPHICS DISCLAIMER

All figures, graphics, tables, equations, etc. merged into this translation were extracted from the best quality copy available.

ABSTRACT Based on plate sheared interference photographs taken of vapor plumes produced by coupling 1.06μm length pulse Nd:glass laser and LY12 aluminium targets, measurements were made that shock wave speeds in air for t<50μs were approximately 473m/s and vapor plume front diffusion speeds were approximately 162m/s. Making use of relevent thermodynamic characteristic equation sets associated with vapor plume plasma, maximum values obtained for ion density, ion temperature, degree of ionicity, and absorption coefficients were, respectively, the results

$$N_i \approx 3.1\times10^{17}\mathrm{cm}^{-3}, T\approx 6096\mathrm{K}, \eta\approx 0.014, \alpha_{(1.06\mu\mathrm{m})}\approx 0.03\mathrm{cm}^{-1}$$

KEY WORDS Laser interactions with materials Plasma diagnosis

I. INTRODUCTION

As far as vapor plumes produced by LY12 aluminum targets irradiated by long pulse lasers are concerned, measurements for the characteristic parameters are important contents associated with studies of destruction mechanisms in laser interactions with materials.

Normally, due to causes in various areas, studies of interferograms are always limited to discussions of refractive indices and electron densities. However, very rarely is their consideration linked up with relevent characteristic equation sets associated with plasma. This article lays stress on going through measurements of air shock wave speeds and corresponding vapor plume pressures produced by the coupling of lasers and LY12 aluminum targets in order to determine pressures associated with interference striation positions. Finally, based on thermodynamic characteristic equation sets related to vapor plume plasma, solution is made for a series of characteristic parameters associated with vapor plumes produced by the coupling of lasers and LY12 aluminum targets.

II. EXPERIMENTAL APPARATUS AND RESULTS

In order to photograph interferograms for changes in refraction indices at different instants produced by the coupling of lasers and targets, use is made of a coordination of wedge dislocation interference and high speed frame cameras. In order to record the process of high speed changes, use is made of ruby pulse laser beams to act as interference light sources.

Under conditions where the lasers hitting targets have energies of 40J, pulse widths of approximately 1ms, and average power densities of approximately 107W/cm2 , interference frame photographs are taken of vapor plumes produced after lasers hit targets--as shown in Fig.2. In Fig.'s, it is possible to clearly see that, in the initial stages of laser and target coupling, air shock waves and aluminium vapor produced by lasers heating target surfaces spray out almost simultanously from target surfaces. Following along with increases in coupling times, aluminum vapor diffusion fronts gradually fall behind air shock wave fronts. Before displacements of datum reference striations in interference striation graphs, one has the appearance of reverse bending. The explanation for this is that vapor plume densities at this location produced sudden changes. That is, a clear region existed between vapor plume fronts and air shock waves. Following along with increases in free oscillation random peak pulses and target coupling times, the axial symmetry characteristics of striations in interferograms were exceedingly bad. In conjunction with this, they were usually accompanied by small particulate shadows. /24

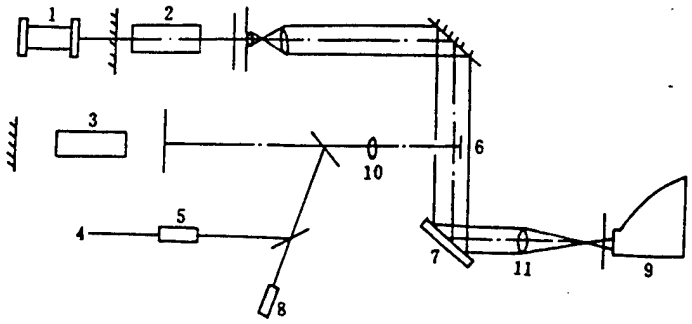

Fig. 1 Optical arrangement for obtain the frame interferograms

1. He-Ne laser, 2. Ruby laser, 3. Nd:glass laser, 4. Oscilloscope, 5. PIN diode detector,
6. LY12 aluminum target, 7. Optical plate, 8. Calorimeter,
9. High speed frame camera, 10. Focusing lens, 11. Lens

Fig.1

(a) 2μs (b) 8μs

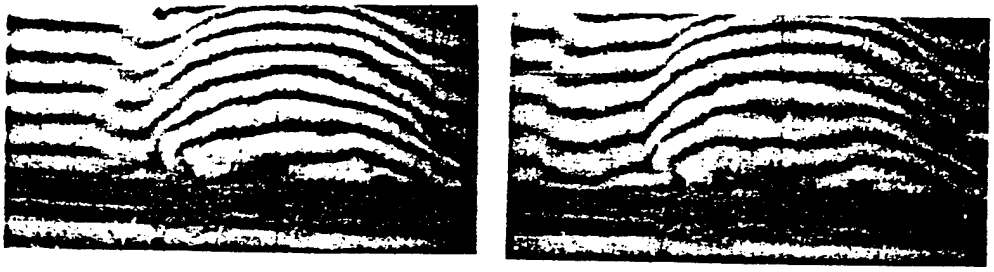

(c) 20μs (d) 24μs

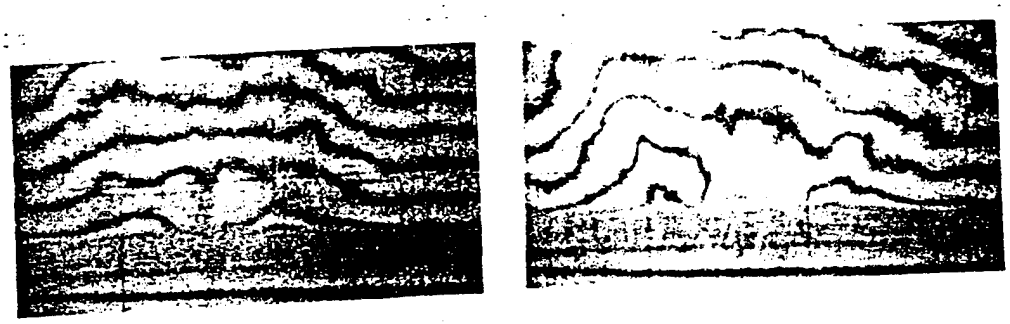

(e) 150μs (f) 172μs

Fig. 2 Typical frame interferograms to show the emission characteristics of the air shock waves and vapor plume front. Laser flux of $10^7 W/cm^2$, aluminum plate thickness of 2mm

/25

Fig.2

III. CALCULATION OF VAPOR PLUME CHARACTERISTIC PARAMETERS

On the basis of interferogram frame photographs associated with vapor plumes produced by laser and target coupling--as shown in Fig.2--it is possible to calculate the change characteristics of air shock wave and vapor plume front displacements as a function of time. With regard to t<50μs, going through measurements for different instants of air shock waves or the distances vapor plume fronts spray away from target surfaces and using least square methods to draw up displacement change relationships as a function of time, one obtains

$$s \text{ shock wave (mm)} = 473t(\mu s) \quad (1)$$

$$s \text{ vapor plume (mm)} = 162t(\mu s) \quad (2)$$

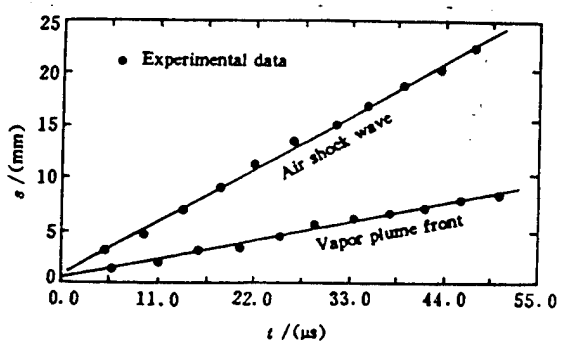

Fig. 3. The displacements of the air shock waves and vapor plume front for $t<50\mu s$.

Fig.3

From Fig.3, it can be seen that air shock wave speeds are approximately 3 times vapor plume front diffusion speeds. The change relationships of their displacements as a function of time are approximately linear.

With regard to the interferograms of Fig.2(d)--making use of Abel transforms and Laplace transforms--it is possible to obtain corresponding vapor plume refraction indices which are [1]

$$\frac{(n-1)}{(n_0-1)} \approx 1 - \frac{1}{2R(n_0-1)}\left(B_0 + \frac{3}{2}B_1 t + \frac{15}{8}B_2 t^2 + \frac{35}{16}B_3 t^3\right) \quad (3)$$

In this, (no-1) = 2.76x10-4 is the refraction index of the surrounding air. λ is the laser wave length of interference light sources. R is the perturbation radius of interference striations. t is the Abel coordinate transform parameter corresponding to interference striations. Bi is the coefficient associated with the use of least square methods to draw up interference striation displacement functions.

Due to vapor plume ionicity being very low, as a result, the contribution of vapor plumes to refraction indices is not only

related to electron density Ne. It is, moreover, also related to the influences of neutral atom density Na and ion density N+ . On the basis of conditions of electrical neutrality associated with vapor plume plasma, it is possible to write the total particle density of a unit volume as

$$N \approx N_a + 2N_e \tag{4}$$

As a result, under our experimental conditions--only giving consideration to the contributions of electrons and neutral atoms--it is, then, possible. Correspondingly, it is possible to write/26 [2]

$$\frac{(n-1)}{(n_0-1)} \approx \frac{N_a}{N_0} - \frac{\omega_p^2}{2\omega^2(n_0-1)} \tag{5}$$

In this, ωp is vapor plume plasma frequency. ω is laser detection frequency. No is a Loschmidt constant. From equation (5), it is possible to obtain corresponding neutral atom density as :

$$N_a = \frac{e^2 N_0}{2\omega^2(n_0-1)m_e\varepsilon_0} N_e + \frac{(n-1)}{(n_0-1)} N_0 \tag{6}$$

In this, e and me are, respectively, the electric charge and mass of electrons. εo is the dielectric constant associated with a vaccuum.

Considering the case of ideal gases, it is possible to obtain the corresponding pressure equation as:

$$p = NKT = (N_a + 2N_e)KT \tag{7}$$

In this, K and T are, respectively, Boltzmann constant and temperature. In order to determine vapor plume pressure p--on the basis of aerodynamic theory--the pressure p1 behind an air shock wave with speed D satisfies the equation

$$p_1 = \rho_0 \frac{2D^2}{\gamma + 1} + p_0 \tag{8}$$

In this, ρo is air density. γ is the adiabatic index of dielectrics. po is ambient pressure. With regard to our experimental conditions, it is possible to select γ = 1.4, ρo = 1.29 kg/m2 , po 105 Pa, D = 473m/s. Corresponding p1 = is approximately 3.4x105Pa.

Considering pressure p1 behind air shock waves, there only exist calibration relationships for recoil pressures associated with plasma on target surfaces during gasification [3] and experimental results [4]. It is possible to work out relationship curves for target surface pressures as a function of vapor plume axial distance (Z). In conjunction, one gets from this pressures corresponding to interference striation positions which are approximatley p=18x105Pa.

If one believes that experimental conditions satisfy Saha equations [5] associated with ionization equilibrium

$$\frac{N_e^2}{N_a} = 6 \times 10^{21} \frac{G_I}{G_A} T^{\frac{3}{2}} \exp\left(-\frac{E_1}{KT}\right) \tag{9}$$

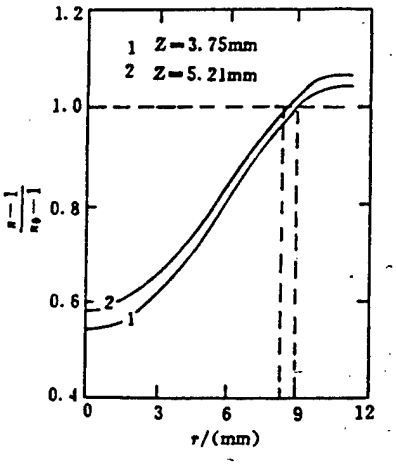

Fig. 4 Distributions of vapor plume refractive index vs r and z

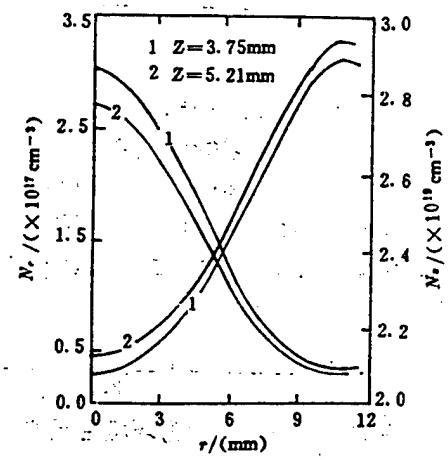

Fig. 5 The density distributions of electron and atom in vapor plume vs r and z

/27

In this, GI and GA are, respectively, statistical weightings associated with ions and neutral atoms. E1 is the first ionization energy associated with corresponding aluminum atoms. By contrast, vapor plume ionicity is

$$\eta = N_e/(N_e + N_a) \tag{10}$$

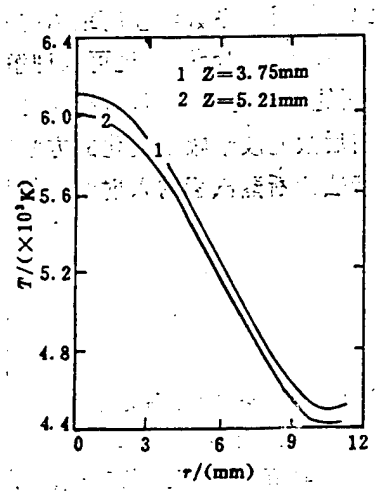

Fig. 6 Distributions of electron temperature vs r and z

Fig.6

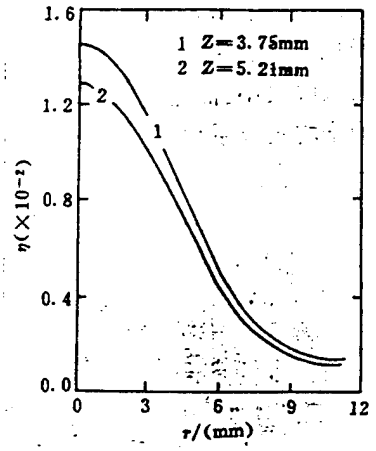

Fig. 7 Distributions of ionicity vs r and z

Fig.7

Due to hω<<KT, consideration is, therefore, only given to the contributions of persistant radiation and that is all. On the basis of Kramer formulae, with regard to partially ionized vapor plumes with laser wave lengths of $\lambda = 1.06\mu m$, it is possible to obtain corresponding vapor plume absorption coefficients in respect to incident lasers [6]

$$a = 1.6 \times 10^{-37} \lambda^2 N_e^2 T^{-\frac{3}{2}} \qquad (11)$$

With regard to the vapor plume interferograms of Fig.2(d), produced by mutual laser and target interactions, from the analyses above, it is possible to obtain change curves as functions of axial and radial distances for corresponding vapor plume characteristic parameters (n-1)/(no-1), Ne, Na, T, η, and α -- as shown in Fig.'s (4-8).

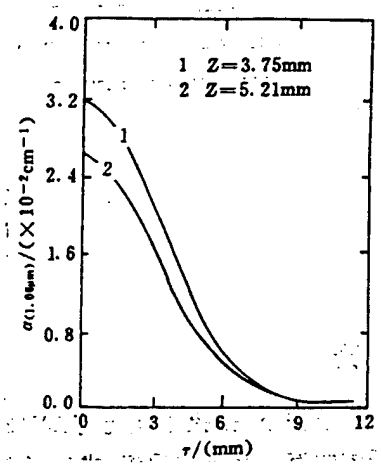

Fig. 8 Distributions of optical absorption vs r and z

Fig.8

/28

IV. DISCUSSION

From the change curve of Fig.9 associated with laser detection wave forms--under the same laser energy densities and through measurements when targets are placed and targets are not placed--it is possible to see that [7] average absorption coefficients associated with vapor plumes produced by lasers--with regard to incident laser energies--reach maximum values when t = 640μs. The values are zero when t < 100μs. Moreover, using interference methods for measurements--on the basis of t = 24μs absorption coefficient change curves as functions of radial distances--it is possible to obtain the average vapor plume absorption coefficient with regard to incident laser energies-- $\bar{\alpha}_{1.06\mu m} \approx 0.01 cm^{-1}$. As far as the initial time phase t<100μs associated with laser and target coupling is concerned, due to the fact that laser energies incident on the surface of targets are not high, vapor plume absorption with regard to incident laser energy is very small. Moreover, going through methods which measure and compare changes in laser wave forms before and after penetrating vapor plume regions in order to determine this small an average absorption coefficient is difficult. This is just explained by the fact that-

-as far as the use of interference methods of diagnosis is concerned--laser plume absorption sensitivities with regard to incident laser energies are very high.

Fig.9

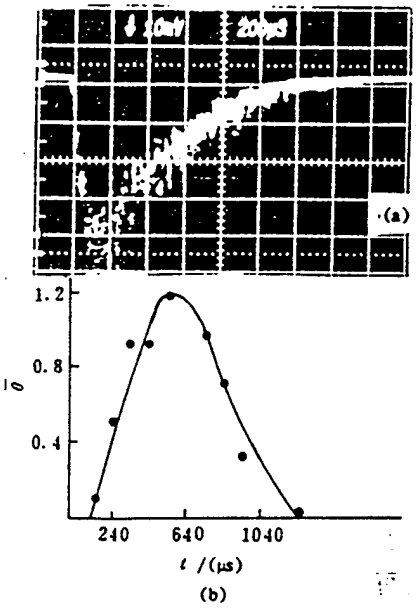

Fig. 9 Absorptivity of the incident laser beam for vapor plume laser flux of $1.6\times10^{7}W/cm^{2}$
(a) The wave shape of laser beam through the vapor plume;
(b) The changes of optical thickness with duration of laser pulse

V. CONCLUSIONS

Under conditions where laser pulse widths are approximately 1ms and average power densities are approximately 107W/cm2 , interference frame photographs were taken of vapor plumes produced by laser and LY12 aluminum target coupling. Use was made of relevent configuration equation sets associated with vapor plume plasma to solve for vapor plume interferograms produced by laser and target coupling. In conjunction with this, characteristic parameters associated with corresponding vapor plumes were obtained.

REFERENCES

[1] Bradly J W. AIAA J,1968,6(6):1190

[2] Maher W E,Hall R B. J Appl phys,1975, 46(2): 762

[3] 孙承纬.强激光引起材料和结构破坏的机理分析.见:激光与材料相互作用的热和力学效应学术会. 上海,1991

[4] 袁永华等.高压物理学报,1990,4(2):114~116

[5] 布克 D L. 等离子体物理常数和公式手册.北京:原子能出版社,1984

[6] Offenberger A A,et al. J Appl phys,1972,43(2):574~577

[7] 刘常龄等.强激光与粒子束,1990,2(3):366~371

DISTRIBUTION LIST

DISTRIBUTION DIRECT TO RECIPIENT

ORGANIZATION	MICROFICHE
B085 DIA/RTS-2FI	1
C509 BALL0C509 BALLISTIC RES LAB	1
C510 R&T LABS/AVEADCOM	1
C513 ARRADCOM	1
C535 AVRADCOM/TSARCOM	1
C539 TRASANA	1
Q592 FSTC	4
Q619 MSIC REDSTONE	1
Q008 NTIC	1
Q043 AFMIC-IS	1
E404 AEDC/DOF	1
E410 AFDTC/IN	1
E429 SD/IND	1
P005 DOE/ISA/DDI	1
1051 AFIT/LDE	1
PO90 NSA/CDB	1

Microfiche Nbr: FTD96C000335
NAIC-ID(RS)T-0076-96